Bachelor degree course
AUTOMATION ENGINEERING
Wels

Compliant Exoskeleton

Submitted as **Thesis**

for the attainment of the academic degree

Bachelor of Science

by

Leopold Hiesmair

Wels, in January 2016

The thesis is advised by

Gernot Grabmair (FH OOE) and Natasha Banerjee (Clarkson University)

Contents

Abstract

An exoskeleton is an external structural mechanism which moves and works with the human joints synchronously. Recent products focus on rigid devices for optimum support of the human body. In order to increase the wearing comfort and the safeness of the ligaments and bends, this paper compares different existing concepts of compliant exoarms, and furthermore creates a new device by combining the advantages and avoiding disadvantages. This comparison includes the analysis of daily tasks, statistical load on each joint and the evaluation of the flexibleness of the device. In addition, the application areas of the concepts are compared in order to create one multifunctional device. The resulting applications range from daily usage for the elderly to therapy of muscles weaknesses to rehabilitation of stroke patients.

Chapter 1

Introduction

1.1 General

Humans have long dreamed of a wearable robot, which fits close to the human body and improves strength, speed and endurance or improve rehabilitation with robotics. Although devices such as wheelchairs and cranes already exist, none of them are flexible enough to be adapted to very different usage scenarios, nor are they fully satisfactory from the point of view of ergonomics and autonomy. For this reason, many researchers are currently working to make universal wearable robots reality. Research in this field has to date yielded various solid exoskeletons, which move and work in synchrony with the human limbs. Most of these are capable of bearing the weight of the wearer and even assisting in the lifting of heavy load. In extreme cases, such an exoskeleton can also replace human muscles or bones. However, this kind of robot has two distinct disadvantages: it is rigid and very heavy, therefore making it difficult to put on. There is in fact a growing family of a different style, that of so-called soft or compliant exosuits, which support or help the human body in individual activities while consuming less energy. This flexible style also protects ligaments, tendons and joints from deterioration. The area of application of such a robot ranges from functional rehabilitation to the restoration of lost functions, such as those of elderly or disabled persons. Another important target audience could be people with muscle weakness or other degenerative illnesses. Such individuals are often severely impeded in performing day-to-day tasks such as holding a glass of water or pulling a chair to sit on. In comparison to a solid exoskeleton a soft implementation has a number of advantages:

- It can be very light and thus have extremely low inertia
- It is easy to put on and to adapt to anatomical variations
- The whole suits is worn slack, so the level of comfort is very high

1.2 Purpose

The aim of this research project is to create one or more sophisticated concepts for a so-called compliant exoarm, which helps people with muscle weakness or other degenerative illness. However, it deals in particular with the human arm to support daily activities, such as holding a glass of water or with rehabilitation methods to rebuild muscles.
For the first concept phase, the undertaking should summarizes all known design concepts, which are state-of-the-art in the field of exoarms. Secondly, different actuators and sensors should be summarized and discussed in order to find the best fitting principal for a compliant exoarm. The desired product should fit the following criteria:

- It leaves the user in full control over his/her movements
- It introduces only minor to no kinematic changes to natural movements
- It assists particular application of the target audience

The project assesses potential devices, to determine if they fulfill the following criteria.

- Should be as small as possible,
- Is easy to wear and use, and
- Has high sensitivity to human motion.

After this project, it should be possible to create a prototype, capable of performing trials on real humans in a daily routine situation.

1.3 Significant Questions

The following questions should be answered in this project:

- Which field of activities should be possible with this exoarm?
- Which human-robot-interaction fits best for the purposed applications?
- Which recent concept best suits the purpose?
- Does it need actuators or sensors? If yes, ...
  - which actuators or sensors have the potential for use in this concept?
  - what is the desired level of sensitivity and accuracy of the components for detecting humans motion?

Chapter 2

Background

2.1 Physical design of a human arm

2.1.1 Overview

The elbow complex serves an important linkage function that enables proper positioning of the hand and the transmission of power from the shoulder to the hand. It consists of three bones: humerus, ulna and radius. However, the arm is composed of three distinct articulations: the humeroulnar joint, the humeroradial joint and the proximal radioulnar joint. These share a common synovial cavity, enabling the forearm to flex, extend, pronate and supinate on the humerus.

2.1.2 Action of the Elbow Complex

Following actions are possible as discussed in [9]:

- Flexion and extension (Figure 2.1-A)
  - **Humeroulnar joint.** Articulation between the trochlear notch of the ulna and the trochlea of the humerus.
  - **Humeroradial joint.** Articulation between the head of the radius and the capitulum of the humerus.
- Pronation and supination (Figure 2.1-B and -C)

- **Proximal radioulnar joint.** Articulation between the head of the radius and the radial notch of the ulna.

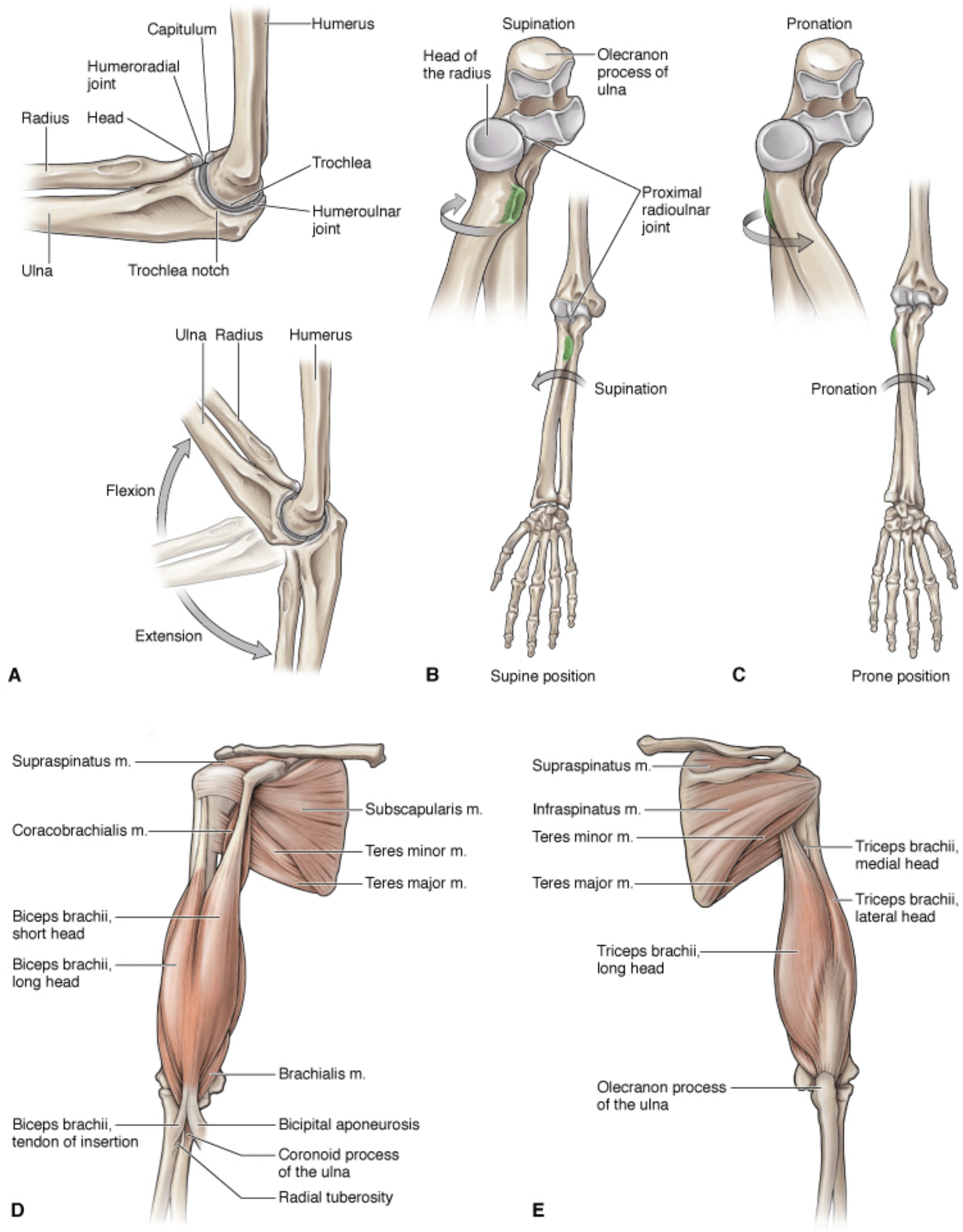

Source: Morton DA, Foreman KB, Albertine KH: *The Big Picture: Gross Anatomy:* www.accessmedicine.com

Figure 2.1: Structure of Elbow Complex [9]

(A) Lateral view of the elbow demonstrating bony landmarks and articulations. Radioulnar joint during supination **(B)** and pronation **(C)**. Anterior **(D)** and posterior **(E)** views of the brachial muscles.

The focus of this project is on extension and flexion of the elbow complex.

2.1.3 Muscles of the Arm

The muscles of the arm (Figure 2.1-D and -E) are divided into to different compartments (anterior and posterior). Each muscle may cross one or more joints. In the following Table 2.1 are all muscles shown with their respective actions.

Muscle	Action
Biceps brachii	Flexion of shoulder and flexion and supination of elbow
Brachialis	Flexion of the elbow
Coracobrachialis	Flexion of the shoulder
Triceps brachii	Extension of shoulder and elbow

Table 2.1: Muscles of the Arm [9]

2.2 Movements Mechanics of the Arm

2.2.1 Flexion Movement

The muscles in the anterior compartment of the arm are primarily responsible for the flexion movement, because of their orientation (Figure 2.1-D). There are two muscle which are attached at different locations to allow the movement.

- **Brachialis muscle**
  Attached between anterior aspect of the humerus and the coronoid process and the tuberosity of the ulna, crossing the anterior elbow joint. The brachialis muscle acts on the ulna (humeroulnar joint), and therefore, it produces flexion of the elbow.
- **Biceps brachii muscle**
  Consists of two heads that attach to the supraglenoid tubercle (long head) and the coracoid process (short head). The biceps brachii muscle converges to insert on the radial tuberosity. The biceps brachii muscle

converges and leads to the radial tuberosity. Because the distal attachment is to the radius, the biceps brachii will also produce supination due to movement of the radioulnar joints.

Full active flexion with both muscles in the normal elbow is until 145 degrees [9].

2.2.2 Extension of the Arm

The muscles in the posterior compartment of the arm are primarily responsible for the extension movement, because of their orientation (Figure 2.1-E).

- **Triceps brachii muscle**
  Consists of three heads. The long head attaches to the infraglenoid tubercle of the scapula, and the medial and lateral heads attach to the posterior humerus. The three heads converge to attach to the olecranon process of the ulna. The long head produces shoulder extension and elbow extension. The other two heads produce elbow extension only.

Full active extention in the normal elbow is until 5-10 degrees [9].

2.3 Muscles Actions during a Movement

The elbow motions of flexion and extension are associated with adduction and abduction motions [9]. For adduction (flexing of the arm), the individual pronates or compresses all anterior compartments of the arm and supinates all posterior compartments. Because of both muscle groups are connected over the attachment to the ulna and radius, the flexion and extention movements are interdependent. Each of them is a complementary motion of the other. The quality of interaction of the anterior and posterior compartments indicates the stability of the elbow. This interaction of the forces is called force couple of the elbow.

2.3.1 Muscle contraction

The tension-generating force and the length changing of the muscle is produced by the activation of the muscle fibers. However, a muscle contraction does not mean muscle shortening because muscle tension can be applied without changes of the muscles length for example in the case of holding a heavy weight. Thus, in order to change the length of the muscle, the contraction has to be concentric or eccentric in the case of shortening and lengthen respectively. Thereby the length changing and the generation of tension are in a relationship [25].

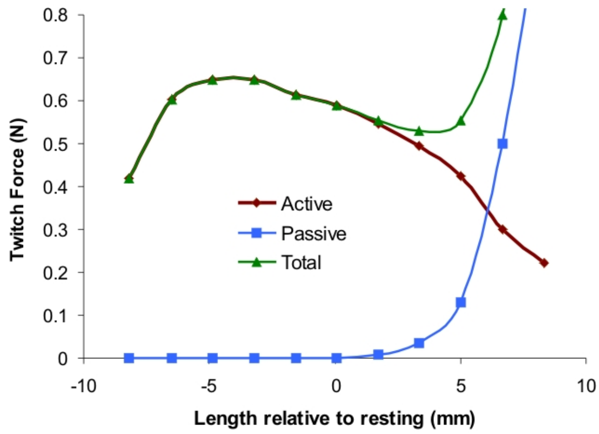

Figure 2.2: Muscle Length-Tension-Relationship [25]

As can be seen in Figure 2.2, the greatest tension of the muscle occurs when the muscles is stretched.

The contraction of the muscle fibers are caused by the motor neurons, whereby one neuron is able to activate more fibers. A single motor neuron introduce a twitch in the muscle fibers. In summation, these twitches superimpose on one another and lead to a forces which produces the contraction of the muscle. The muscle fibers and the nerve axon, where the motor neurons derive, together are called motor unit. The mentioned twitches, which seam like fast contraction and relaxation, produce electric potential variations. These motor-unit potentials least from 5 to 20 ms with an amplitude between $+200\mu V$ and $-200\mu V$ [4].

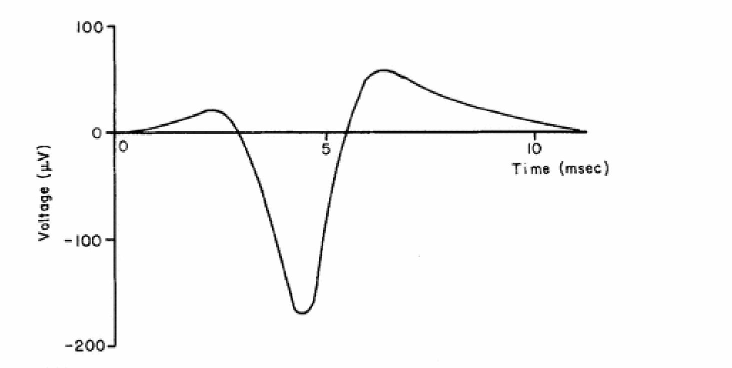

Figure 2.3: Typical motor-unit potential [4]

In Figure 2.3 can be seen a typical motor unit potential which is called the **myoelectric signal**. If a considerable amount of such signals are superimposed, it results in the electromyography signal (EMG signal) which can be detected by electrodes sitting on the skin above the muscle. In Figure 2.4 can be seen an example of detecting the activity of a muscle with example signals [20].

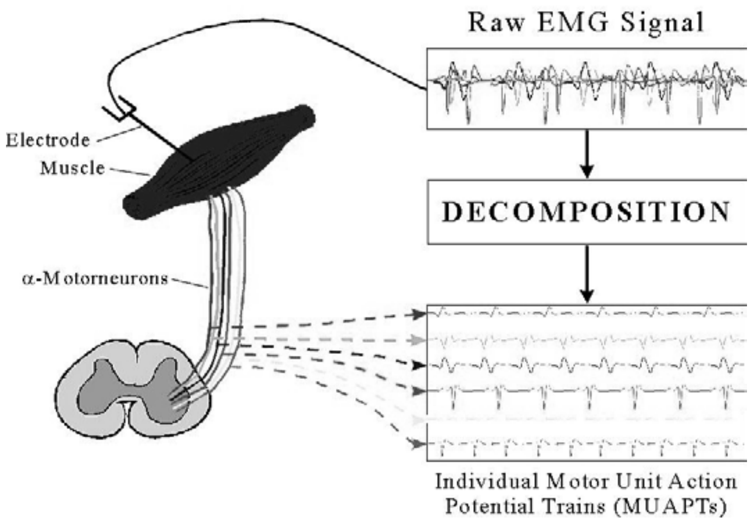

Figure 2.4: EMG signal and motor-unit potentials [20]

2.3.2 Movement Example

A movement example can be illustrated in flexioning an elbow with a certain resistance (weight). The humeroulnar joint illustrates the fulcrum (axis). By pronate the bizeps muscle (compress) accrues a force to the radius bone. As shown in Figure 2.5, the movement is simplified with a force lever in third class (the effort is between the pivot and the load) [1, Page 15].

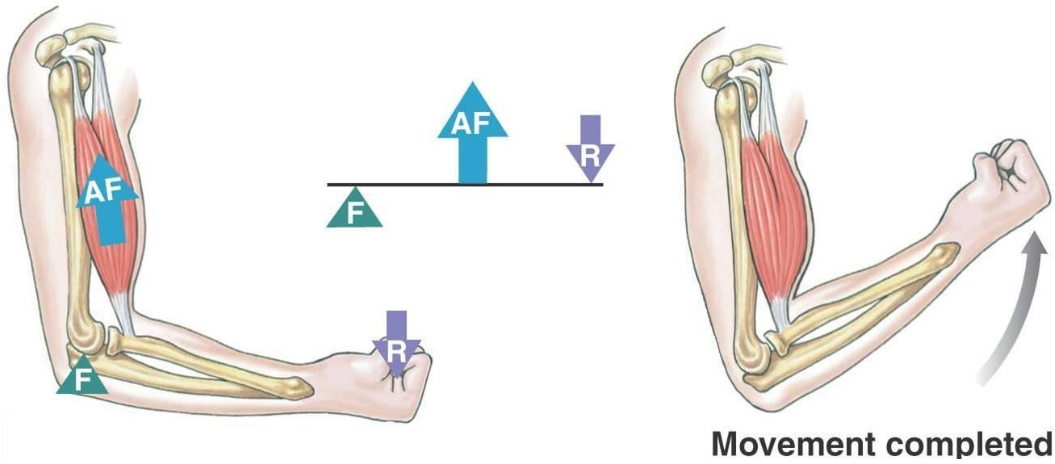

Figure 2.5: Example of lifting a weight [1]

2.4 Activities of Daily Living - ADL

In order to understand the typical loads on the joint during ADLs, it is necessary to analyze these activities with a motion capture system. 19 activities were captured and evaluated in the following categories: general reaching tasks, functional tasks, eating and drinking, and hygiene-related tasks.
As an Figure 2.6 can be seen, a 7-DOF model of the human hand is with the shown frame assignments. The torques were calculated with two different methods: a modeling simulation package (Cosmos/Motion, Solidworks) and an analytical approach (Autolev, Online Dynamics).

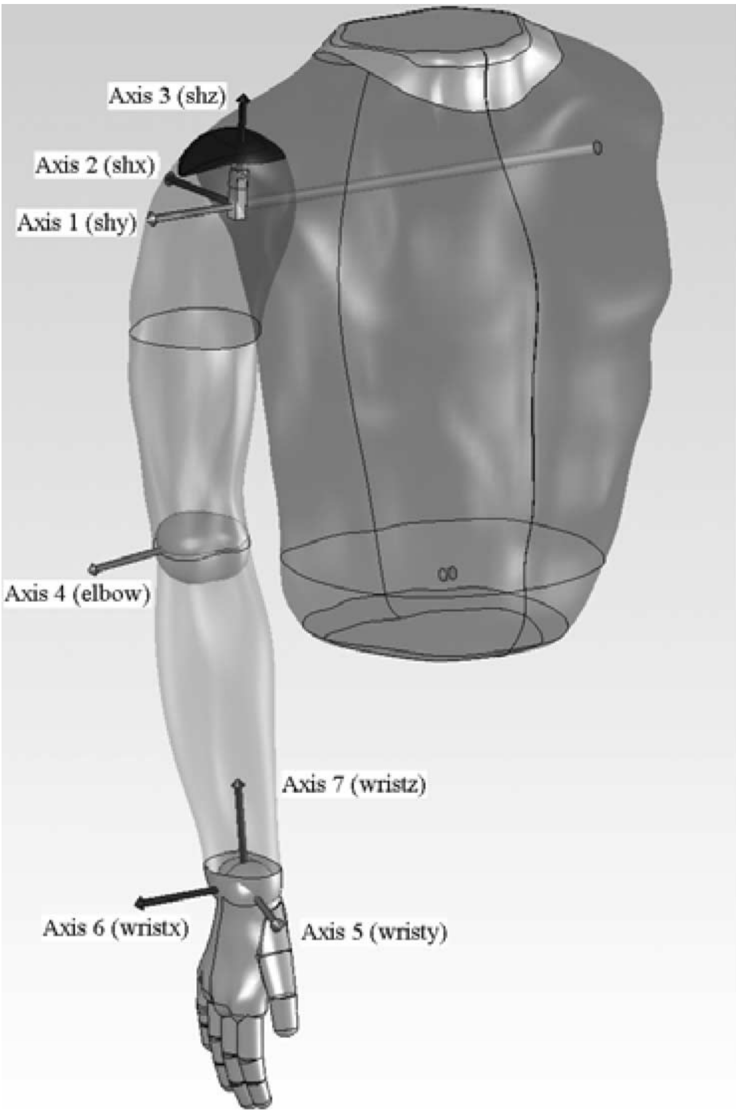

Figure 2.6: Assignment of Euler Y-X-Z axes for the Vicon system [19]

The calculation of the torques and the most used angles resulted in the Figure 2.7. The upper plots represent the statistical distributions of the human arm ordered by the regarding joints. The bottom plots illustrate the torques of the regarding joints during the 19 ADLs. The zero position of the plots can be seen in Figure 2.6.

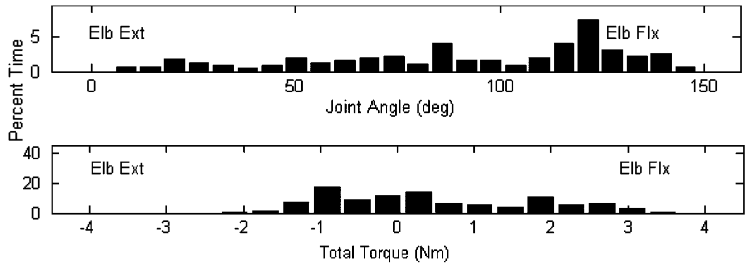

Figure 2.7: Statistical distribution of human arm joint angles (top) and joint torques (bottom) during 19 ADLs [19]

The first interesting parameter in the Figure 2.7 is the **joint angle** of the elbow joint. The distribution shows a trimodal form with the peak on about 145° which means that this angle is most commonly used during ADLs but with only 6% . Despite of the a few other peaks, the distribution is relatively constant in comparison to all other joints. That follows to the assumption, that the whole range of the joint has to be assisted because all angles between 5° until 150° are used in ADLs.
The second important focus is on the **total torque** of the elbow joint. While evaluating the resulting distribution for the elbow joint, the almost constant torque distribution is noticeable. The total torque in the elbow joint ranges from −2 Nm until 3 Nm while about 80% off all load occurs between −1 Nm and 2 Nm.

Based on the results of the ADL evaluation, the Figure 2.8 indicates the requirements on each axis for an assistive robot.

		VICON AXIS						
	MEASURE	1	2	3	4	5	6	7
Anlge (deg)	ROM	110	100	135	150	115	70	150
	Mean	42.0	35.4	13.1	92.1	3.1	-4.8	11.7
	Median	35.1	41.4	9.1	98.6	3	-9.3	15.9
Torque (Nm)	Mean	3.5	1.0	-0.3	0.45	-0.02	0.04	0.00
	Median	3.9	0.4	-0.1	0.18	-0.02	0.02	0.00
	RMS	4.4	1.6	0.7	1.4	0.07	0.11	0.01

Figure 2.8: Kinematic and dynamic joint design requirements [19]

Again, the elbow axis which is shown as number 4 is evaluated. The Figure 2.8 shows under the row 4 of the vicon axis the statistical values of the elbow joint for the angle and total torque which are minimal required to be supported by the exoskeleton. The significant values of this table are the RMS torque of 1,4 Nm and the mean angle of 92,1° [19].

Chapter 3

Methods

3.1 Human-robot interaction and Actuators

The following three sections describe the basic principles on how an assistance robot can be designed which includes the interaction with the human as wells as different actuator types.

3.1.1 Human-robot interaction (HRI)

As the exoskeleton moves synchronously with the human joint, an effective HRI is very important. Therefore, the location where the robot comes in contact with the human skin is very important because it has a high influence on the quality of the measurements. Existing projects use skin elements that reduce pain to improve comfort, safety, and transfer of load force.

Types of HRI are:

- **Haptic interface**
  Touch and force sensors on the human skin capture the movement and give feedback. This mechanical stimulation can be used for a remote control for mechanical devices or virtual object.
  As an example for haptic interface, Kapur et al. [13] developed an exoskeleton using vibration actors at different points of the patient's skin.

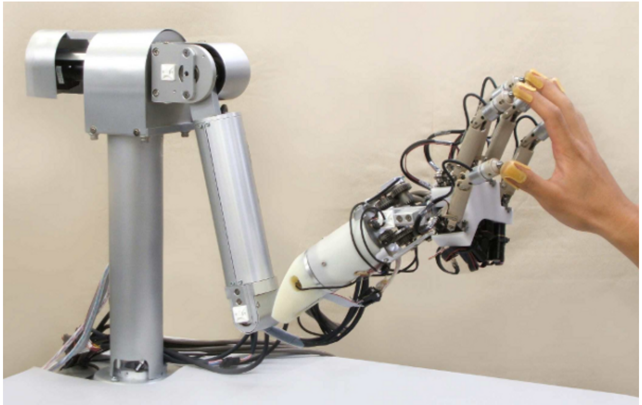

Figure 3.1: Haptic interface example [11]

- **Electromyograph (EMG) Signal Detection**
  EMG sensors attached onto the skin above the muscle detect naturally generated muscle signals. This enables an interface which is independent of the individual user and their weaknesses and illnesses.
  As an example for an EMG detection system, Myomo Inc. introduced the MyoPro as an upper limb orthosis [17].

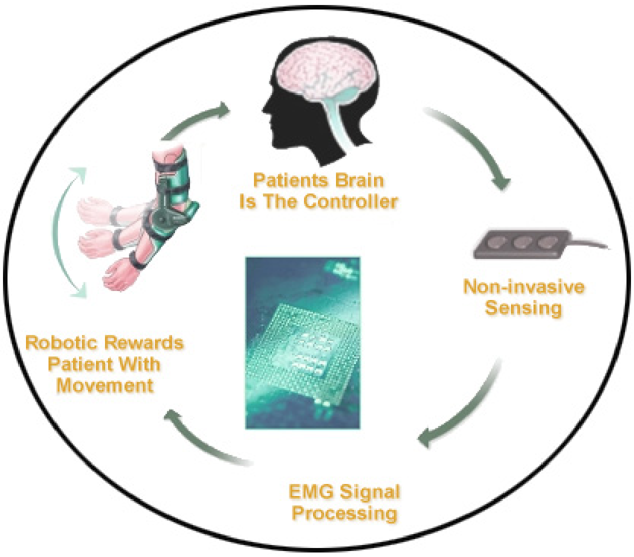

Figure 3.2: EMG interface signal flow [17]

The detected EMG signal consists of superimposed signals from different motor units at a time. As shown in [20], the EMG signal is analyzed to gather information about the biomedical state of the muscle.

- **Visual interface**
  This interface uses cameras to capture gestures (face or mouth) and processes commands. Motion and gestures capture is often used for virtual gaming.
  As an example for visual interface, Baklouti et al. [2] proposed a face and gestures controlled exoskeleton.

HRI Discussion

As already mentioned, this project propose to create a new sophisticated concept for an exoskeleton which assists the human elbow in daily life as well as rehabilitation. Hence, an innovative method has to be set at first.
A **visual interface** as controlling unit is a innovative way to collect the proposed movement of the patient. In addition, no sensors would be needed in the exoskeleton. However, the capturing with cameras and the processing of the gestures needs lot of resources which has a negative impact on the portability of the device.

In terms of feedback, **haptic interfaces** have significant benefits. Force sensors demonstrate a simple method of detecting the desired movement of the patient. Additionally, feedback on the human skin can be simply realized which enables a stimulation function of the exoskeleton. The minimal processing of data is another advantage in comparison to other interfaces.However, since the force sensors are based on detecting motion, the haptic interface requires an initial movement patient's arm moving without the exoskeleton. This leads to a significant disadvantage for patients who cannot perform significant self-motions of the arm, and who do not have assistance in performing the initial motion.

In comparison to the visual and haptic interfaces, the **EMG detecting system** has several benefits. If the EMG sensors are attached close to the human skin above the muscle, already weak muscles are measurable and processable which increases the accuracy and reduces the latency. Furthermore, in comparison to the haptic interface which necessitates arm motion, the EMG sensors can detect and process natural muscle signals before contraction or relaxation. Consequently, the muscle and the assistive robot move synchronously. While the muscle does not move due to weakness, the signal is still present, and the exoarm continues the movement and completes the desired movement until the patient needs to stop motion. This leads to a useful tool even for weak patient because no motion is needed to actuate the exoskeleton. Additionally, this system enables the exoskeleton for different individuals to be independent.

3.1.2 Actuation

Electric Motor

Traditional robots use usually electric motors [3] with gear boxes to drive their components. Exoskeletons made of traditional robotic technology are stiff and supply large torques. As the electric motor in wearable robots is not flexible to provide injuries, such methods require a compliant motor control algorithm. Such algorithms for actively control of compliance are already developed by Salisbury [21] and Paul [18].

The following list concludes the advantages and disadvantages of the electric motor as an actuator:

Advantages

- accurate movement in term of position and velocity
- easy to control
- simply attachment

Disadvantages

- very stiff
- difficult to implement compliant controlling algorithm

Smart Materials

Smart materials have one or more special properties that can be changed by an an external stimulus. This stimulus can be stress, temperature, moisture, pH, electric fields or magnetic fields. In the field of robotics, the most common

types are electroactive polymerier (EAP). This smart material converts the energy of an electric field into the mechanical energy of a change in distance, or strain.
There are already existing concepts which use EAPs as artificial muscles in order to model the human arm. [22]
The group of EAPs includes two different types:

- **Electronic EAP** - driven by electric field
  exhibits high mechanical energy density with high required voltage (>100MV/m), and holds the strain with DC voltage
- **Ionic EAP** - diffusion of ions
  bi-directional actuation with a low required voltage (1-2 V)

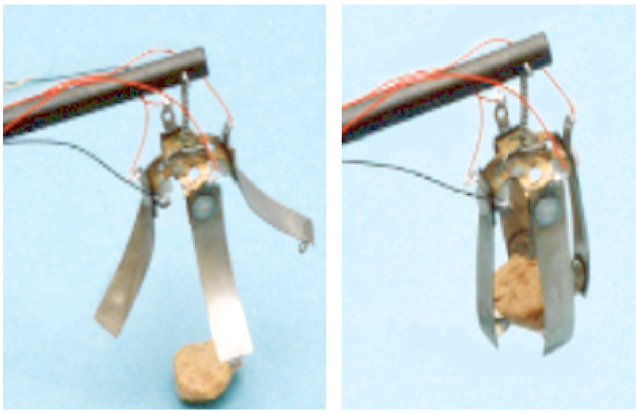

Figure 3.3: 4-finger EAP gripper lifting a rock [22]

As an example, De Rossi et al. developed a kinesthetic system with EAP actuators Example for using EAP [7].

There are many approaches to create **passive exoskeleton** which use only force generating actuators. However, these designs cannot actively assist movements, which limits the application significantly. Typical passive exoskeletons use springs to negate the effect of gravity so that the patient only needs little effort to move the arm.
The following points show the advantages and disadvantages of smart materials as an actuator of a assistive robot:
Advantages:

- tiny construction possible
- innovative design
- easy to control

Disadvantages:

- materials which create enough torque are not developed yet
- difficult to manufacture

Pneumatic Muscle Actuator - PMA

The majority of the existing concepts uses electromagnetic motors. Hence, recent approaches [16] focus on the usage of artificial muscles such as pneumatic muscles actuators (PMA). In comparison to an electric motor, PMAs are only able to generate tension force, therefore, PMAs are often used as a pair to generate a bidirectional torsion. They mimic the biceps and triceps in a human arm, i.e., when one contracts, the other relaxes and vice versa. This actuators reach length changes by contraction similar to the human muscle. The contraction of the PMA is caused by entering air pressure in an elastic tube. The Figure 4.4 shows one inflated PMA, where the noticeable length reduction in comparison to the nominal length can be seen, and another one PMA in nominal length.
The following advantages and disadvantages summarize the key points of the PMAs as an actuator in an assistive robot:
Advantages:

- better forces-to-weight ratio
- ability of compress the air enables flexibility safeness of the exoskeleton

Disadvantages:

- non-linear characteristic is difficult to control
- low bandwidth with 5 Hz

Experiments with PMAs have shown the dynamic behavior while releasing a 30kg mass at different pressures which can be seen in Figure 3.4 [14].

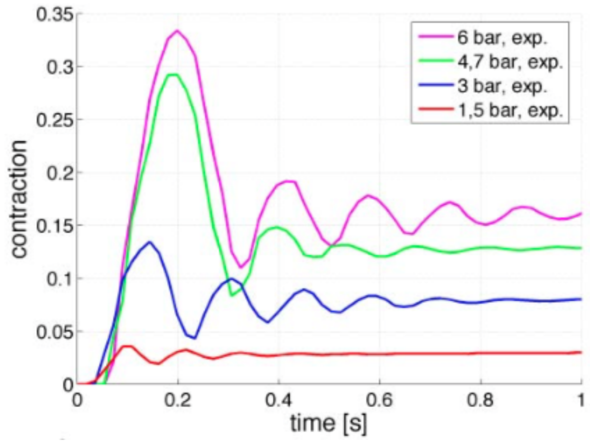

Figure 3.4: Release of 30kg mass with different pressures [14]

At time t=0, the PMA is in its nominal length for all pressure levels. When the mass is released, the actuator changes the length immediately regarding of the pressure level. This leads to a compliant behavior of the muscle especially at the maximum pressure of 6 bar. The contraction of the PMA changes with a certain oscillation which is proportional to the pressure level.

Actuators Discussion

Traditional robots are usually very stiff and can apply very high torques which can result in injury of the users. Hence, the resulting concept will be applied for rehabilitation and daily life where the safeness has to be very high. In order to gain safeness of the device, the following points have to be adhered to:

- Only apply as much torque as is required
- User decides all motions of the exoskeleton
- Compliant motion of the robot

A considerable amount of recent assistance robots are driven by **electric motors** because of their broad application possibilities. However, an electric motor with a traditional control is stiff and can apply very high torque with less energy which can lead to injury of the user. To get a the required compliance,

the electric motor has to be compliantly controlled.
Algorithms for compliant control of stiff actuators may prove complex, and if not tested thoroughly, may yield errors that prove hazardous to the patient. Instead of having a stiff mechanical design and a compliant control, a better approach is to use a compliant mechanism. Pneumatic muscle actuators implicitly provide compliance, and do not require compliant control algorithms.

PMAs are an innovative concept of driving a robot because of the analogy to the real human muscle. These actuators have a high force-to-weight ratio which enables a lightweight design of the robot and a higher level of comfort. Additionally, PMAs allow treating the force control loop as a position control where the change in muscle length is nearly proportional to the force applied, as can be seen in Figure 4.8.

Recent research is focused in **smart material** because it enables particularly tiny designs of the robot. However, the requirement of compliance is fulfilled besides the research on these materials are in the initial state which makes it difficult to gain information and samples for experiments.

3.2 Existing Concepts

3.2.1 Introduction

In this chapter existing concepts of exoskeletons are described and discussed. This section summarizes existing state-of-the-art design concepts. In order to compare these concepts, its important to answer significant questions, such as:

- Who is the target audience?
- Which field of activities should be possible?
- How many degrees of freedom (DOF) are needed?
- Which flexible actuators and sensors are needed?

During the literature research, all collected concepts were evaluated based on the significant questions.
The following concepts have been evaluated:

- Armeo products (Hocoma AG, Switzerland) with 7 DOF
  - Active exoskeleton - ArmeoPower
  - Passive exoskeleton (Springs) - ArmeoSpring
  - sling suspension system - ArmeoBoom
- ARMin 3 exoskeleton
- MyoPro arm brace (Myomo Inc., Cambridge MA) with 1 DOF for elbow joint; EMG control system
- Hand Mentor (Kinetic Muscles Inc., Tempe AZ) with 1 DOF for wrist and fingers; actuated by air muscles
- Robo Suit HAL-5 (Cyberdyne Inc., Japan) is a full body exoskeleton for disabled; uses EMG signals
- RUPERT IV with 5 DOF for elbow joint; driven by pairs of PMA

By answering the mentioned significant question, the number of fitting concepts to the aim is reduce to the following two devices.

3.2.2 RUPERT

RUPERT [3] [23] in the fourth generation is developed for robot assisted upper extremity repetitive therapy. This device has five actuated DOF driven by artificial pneumatic muscles (PMs) at the shoulder, elbow and wrist. Therefore, the movements are flexible which minimizes hazard to the joints, ligaments and tendons. RUPERT is a low-cost device, and is easy to use and wear and is designed to be used for daily activities, therefore, it is lightweight which makes it portable.

Design

RUPERT is designed with four pneumatic muscles to achieve the desired range of motion. These pneumatic muscles actuate the shoulder elevation, elbow extension, supination and wrist extension. To enable the best usage for different patients, multiple adjustments are added to supply multiple sizes. RUPERT is designed without compensation for natural gravity in order to keep the device realistic for real-life activities.

Figure 3.5: RUPERT IV [3]

Control

The control of RUPERT is based on a cascade closed loop control with an inner loop (individual joints) and an outer loop (level of functional task). The closed-loop controller is developed for a passive therapy mode (designed in MATLAB/Simulink). The desired movements are predefined by the therapist. If the patient starts the sequence and does not reach the defined end position, the muscles are activated. In addition, the therapist is able to change the amount of the movement as well as the speed of the movement according to the condition of the patient. This activation sequence of the muscles is calculated using the SIMM model [1] for each activity.

Results

RUPERT provides a five degree-of-freedom exoskeleton, with a closed-loop controller. In order to minimize hazard to the joints and ligaments RUPERT uses PMs for flexible movements. The adaptive controller enables the operation of different users.

[1] http://www.musculographics.com/html/products/simm.html

Unfortunately, this device supports only programmed repetitive activities. Consequently, all movements have to be defined and programmed which which may not be useful in daily life.

3.2.3 MyoPro

MyoPro [17] is a portable lightweight and electric motor-driven brace which enables individuals to initiate and controls arm motion. MyoPro, developed by Myomo Inc. [2], uses the patient's own muscle signals to move the arm and is therefore useful for patients with any kind of weakness or illness such as stroke, multiple sclerosis (MS), amyotrophic lateral sclerosis (ALS), brain and spinal injury and other neuromuscular disorders. When the user tries to move the arm, the sensor system activates the motor to move the arm in the desired direction. During this movement, the brace amplifies the weak muscle signal to help bend and move the user's arm.

Figure 3.6: MyoPro myoelectric limb orthosis [17]

Design

MyoPro has a rigid shell with elastic stripes to fix the arm in the desired position. An EMG (electromyography) control software detects even very weak muscles signals created by the user in order to move the arm. This data is processed to obtain activations for the electric motor on the device to enable the desired movement of the arm. This processing occurs so quickly that it is not apparent to the patient.

[2] http://www.myomo.com

Results

This upper limb orthosis assists patients with any kind of weaknesses and illnesses in daily activities. The EMG control system enables easy use of MyoPro without any preparation of the desired movements for different individuals. While the electric motor is accurate, it may cause stiffer movements compared to MyoPro.

3.3 Modeling

3.3.1 Introduction

This section summarizes the modeling of the human arm as discussed in the approach of Tzong-Ming Wu et al. [26] on developing a muscle-strengthening exoskeleton.

3.3.2 Create Kinematic Model

As discussed in the previous chapter, the human arm is separated into the upper limb and the forearm. The upper arm is from the shoulder joint (glenohumeral) to the elbow joint and the forearm connects the elbow joint with the palm of the hand (Figure 3.7). The lengths of the respective parts are different across various human subjects. As shown in Figure 3.7, the length of the upper arm bone is referred to in [26] as r_{SE} and the length of the forearm bone as r_{EH}. As this project is focused on the elbow joint, the upper arm is mostly in a neutral position and therefore not influenced by the gravitation and can be neglected for this part. Hence, this segment can be modeled as a two-link linkage. The geometry of the human body is assumed as symmetric so keep the model simple. Also the weights of the arms are set on the center lines of the respective segments with m_f and m_u. Furthermore, the mass of the hand is ignored, because it does not effect the model in comparison of the mass of the other two parts.

To model the human arm, the authors of [26] use the Denavit-Hagenberg parameters [8]. This leads to four Cartesian coordinate systems 0-4, where in this case system 0, which is attached on the ground as a reference system, to system 3 stay static. All parameters in Figure 3.7 are created based on the definition of Denavit-Hagenberg notation.

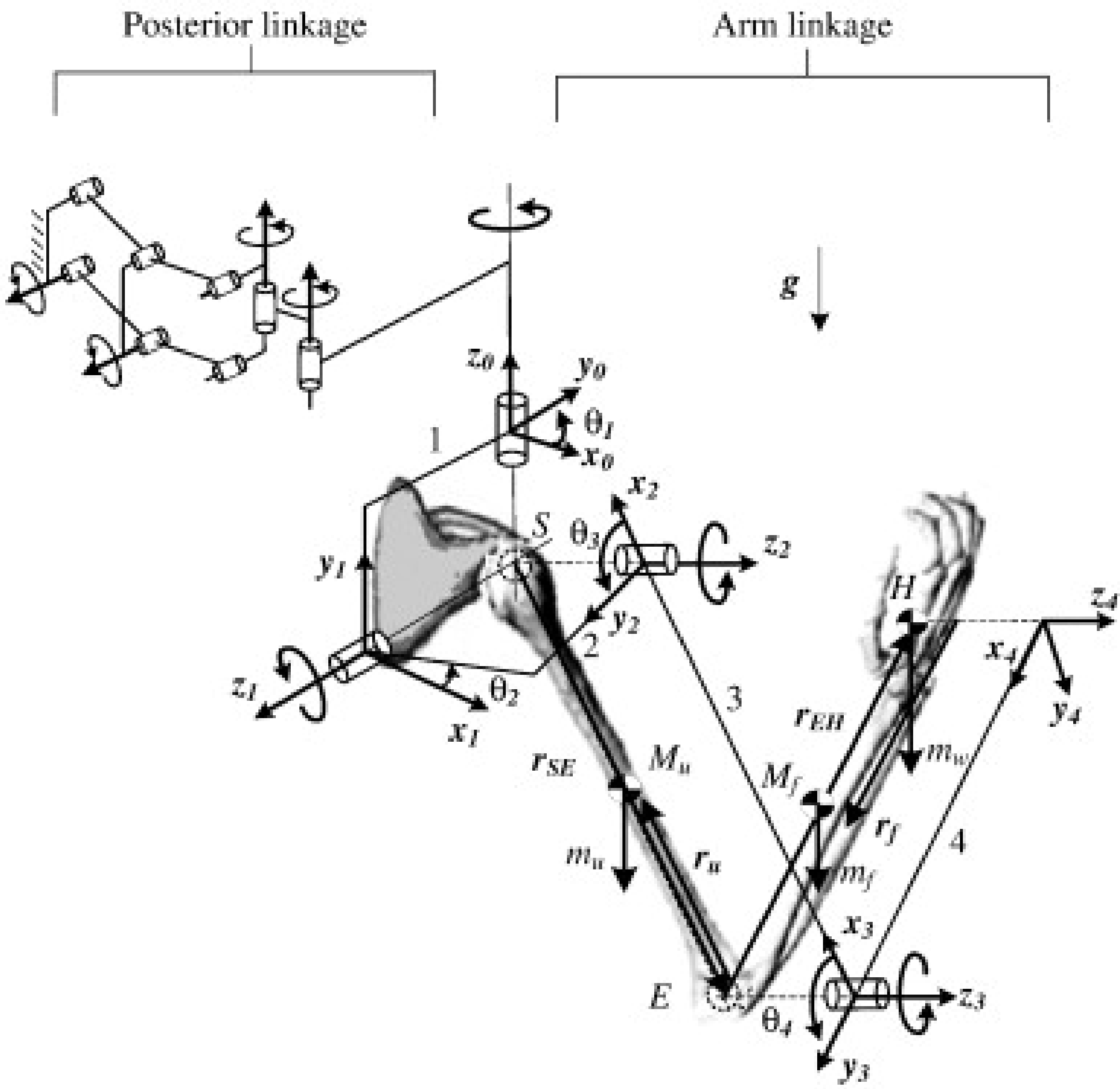

Figure 3.7: Kinematic model of human upper limb [26]

3.3.3 Calculate of strain during lifting

To evaluate the robustness of the device, its important to know the strain during a lifting exercise, for instance, a free-weight lifting. In this exercise, the muscle is trained by repetitive lifting and while increasing the weight gradually. As in Figure 3.7 shown, the load is called m_w and is located at the palm of the arm at the point H. The masses of the upper arm and the forearm are constant and are in the mass center of the respective parts. Therefore, the potential energy can be calculated as followed:

$$V_g = -m_u \mathbf{g} \cdot (\mathbf{r_{SE}} + \mathbf{r_u}) - m_f \mathbf{g} \cdot (\mathbf{r_{SE}} + \mathbf{r_{EH}} + \mathbf{r_f}) - m_w \mathbf{g} \cdot (\mathbf{r_{SE}} + \mathbf{r_{EH}}) \quad (3.1)$$

The vectors r_u and r_f in Equation 3.1 can be split up into $r_{u,x}$ and $r_{f,x}$, whereas the other components $r_{u,y}$, $r_{u,z}$ and $r_{f,y}$,$r_{f,z}$ are neglected. This provides the equation:

$$\begin{aligned} V_g = [&-m_u g \cdot (r_{SE} + r_{u,x}) - (m_f - m_w) g r_{SE}] \sin\theta_2 \cos\theta_3 \\ &-[m_f g (r_{EH} - r_{f,x}) + m_w g r_{EH}] \sin\theta_2 \cos(\theta_3 + \theta_4) \end{aligned} \quad (3.2)$$

The torque in the joint can be calculated with the equation:

$$\tau = \frac{\partial V}{\partial \theta} \quad (3.3)$$

As the device in [26] focuses on the elbow joint, the torques of other joints are not shown. Therefore, the derivation is only used for θ_4.

$$\tau_{twist} = [m_f g (r_{EH} - r_{f,x}) + m_w g r_{EH}] \sin\theta_2 \cos(\theta_3 + \theta_4) \quad (3.4)$$

This special twist torque has to be prevented by the developed device. Although, the torque supported by the actors of the device is a different one, but can also be calculated with the same model.

The maximum of the torque during a lift occurs when the upper arm is in a vertical position. That means that $\theta_2 = 0\,\text{deg}$ and $\theta_3 = 90\,\text{deg}$. So follows the equation for the lifting torque strained on the elbow joint.

$$\tau_{lift} = [m_f g (r_{EH} - r_{f,x}) + m_w g r_{EH}] \sin\theta_4 \quad (3.5)$$

The Equation 3.5 has its maximum at $\theta_4 = 90\,\text{deg}$ and further only depends on the masses of the arm and the external weight.

$$\tau_{lift,max} = m_f g(r_{EH} - r_{f,x}) + m_w g r_{EH} \tag{3.6}$$

Chapter 4

Exoskeleton Concept Provided by Thesis

4.1 Introduction

The main purpose of this research is to develop a new sophisticated and unique concept of an exoskeleton for an application in rehabilitation and activities in daily living (ADL). While the previous chapter summarize the background information and state-of-the-art techniques, this chapter compares different methods, combines the methods, calculates required parameter and results in a raw design. The new concept is designed in the 3D CAD software Autodesk Inventor Professional.

4.2 Main Decisions

Based on the discussions in prior chapters on the advantages and disadvantages of different exoskeleton approaches, a novel exoskeleton concept is designed in this chapter. By taking the existing concepts into account, different main decision can be formed.

As discussed in Chapter (3.1.1 Human-robot interaction), the haptic and visual interfaces have disadvantages for use in rehabilitation and ADL applications. The EMG detecting system has serious benefits in terms of multifunction, accuracy and real time processing.

In order to realize the required compliance, the pneumatic muscle actuators fit best for a compliant exoskeleton due to the compressibility of the air which drives the PMAs. As can be seen in Figure 3.4, PMAs show compliant behavior even at maximum pressure, which proves beneficial in comparison to electric motors.
Finally, the advantages of two existing concepts, RUPERT and MyoPro, were combined to provide a new compliant design for an exoskeleton which can be applied for different individuals in a wide range of situations. The new design developed in 3D CAD software assists the human elbow to lift objects.

This leads to an exoskeleton **controlled by EMG sensors** and **driven by PMAs** with **one DOF** while restricting no other DOF of the human arm which enables a **comfortable and easy-to-wear device**.

4.3 Comparison of Actuators and Sensors

4.3.1 Sensors

As discussed in Chapter *3.1.1 Human-robot interaction*, **EMG detection system** allows the robotic system to assist the patient in performing desired motion by sensing muscle contractions, relaxations, and natural muscle state. This allows the robot to power the arm in real time without any delay because the stimulation of the muscle and the processing of the signal data take place simultaneously and enables a humanlike device with is adaptable for any user. According to surface EMG, electrodes are attached on the skin above the muscle for recording information present in the muscle. The attached electrodes pick up the EMG signal and modify it with a differential amplifier.
The estimated use of EMG detection causes following issues [15]:

- the natural generated EMG signal varies even in the same motion
- the activity level of each muscle are different across subjects
- one muscle is involved in various motions
- the role of each muscle differs and various angles and positions of the limb

- signal-to-noise ratio is high

To cope with these issues, biomedical instruments was developed to process the raw EMG signal. Since the raw signal of the electrodes has low voltage amplitudes and carries noise, it is necessary to filter and amplify the signal. Yen et al. [27] developed an integrated circuit (IC) design which extracts the information using three stages: instrumentation amplification, gain control and filtering.

Another chip design has been developed by Kajitani et al. [12] for autonomous mobile robotics. The logic circuit can be adapted according to the desired muscle. Additionally, the inbuilt CPU core, which uses a genetic algorithm, provides fitness calculation based on the user's activities. This is useful to record muscle behaviors during rehabilitation. Recent myoelectric prostheses are already equipped with this chip for data acquisition and processing.

The raw EMG signal consists of a number of superimposed motor unit signals or myo-electric signals. As such, for the signal to be useful, information about the muscle action needs to be extracted. Since the interesting information is the amplitude of the signal, the root mean square (RMS) is calculated to gain useful data:

$$RMS = \sqrt{\frac{1}{N}\sum_{i=1}^{N} v_i^2} \tag{4.1}$$

In Equation 4.1, N stands for the number of samples, v_i the measured voltage of the ith sampling. Before assuming the activity of the muscle, the basic signal level has to collected to calibrate the controller.

In addition to the EMG sensors, force and angle sensors are attached on the elbow joint to measure the torque and velocity created by the user. This enables the device to decide if the motion needs to be supported or not.
The two sensor system leads to different scenarios:

- **EMG signal level is low - torque sensor signal is high**
  the user moves the limb with low contraction of the muscle
  $\rightarrow$ no activation of assistive actuators
- **EMG signal level is high - torque sensor signal is low**
  the user tries to move the limb with high contraction of the muscle but

the limb does not move
→ activation of assistive actuators

- **both signals are low**
  the user relaxes the limb or move very slowly
  → no activation of assistive actuators

- **both signals are high**
  the user moves the limb with high contraction of the muscle
  → no activation of assistive actuators

These decisions enable the user to perform self-motions of the limb as far as possible without robot intervention.

In oder to calibrate the controller, the standard parameters, such as the standard EMG signal level of the relaxed muscle, have to be collected. Therefore, the user performs typical daily life motions for calibration. Using these motions, the factor between the EMG signal level and the torque sensor signal can be evaluated to enable the mentioned decisions. During the estimation of this factor, the RMS values of both signal are subtracted. This resulting error value become zero if the generated robot motion and the user's motion are the same.

Previous approaches [15] have provided analysis of the correlation of the EMG signal and the joint angle with human subjects while lifting a dumbbell (5 kg).

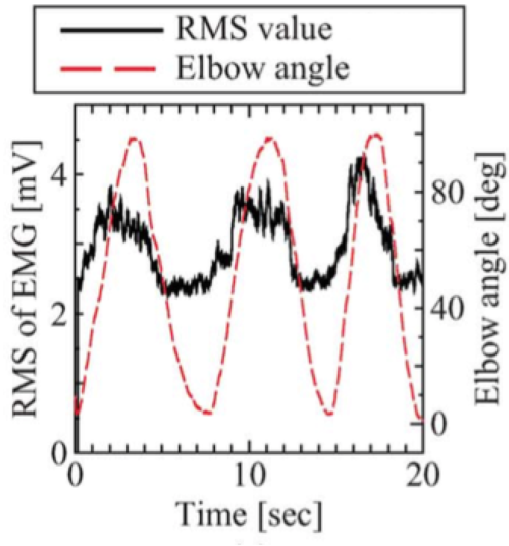

Figure 4.1: Experimental result of lifting a weight [15]

As shown in Figure 4.1, the actual angle of the elbow joint and the detected RMS value of the EMG signal on the biceps are in relation with each other.

4.3.2 Actuators

Based on the previous decisions of using PMAs to drive the exoskeleton, the following part discusses the characteristics of two different PMA types which are Plated Pneumatic Artificial Muscle (PPAM) and McKibben muslces of Festo (Festo Fluidic Muscle).

The use of PMAs have been significant increasing due to their humanlike characteristic such as variable-stiffness, physical flexibility and very high energy-to-weight ratio [24].

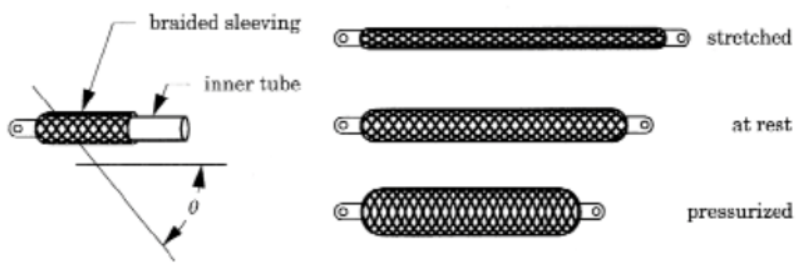

Figure 4.2: Example of McKibben Muscle [24]

Figure 4.2 shows an example of a McKibben muscle in different stages. It consists of a rubber inner tube which expands when air pressure is applied. The outer braided sleeve limits the radial extension of the inflation and transfers the tension. These muscles are usually driven with pressures from 1 to 6 bar and more.
The second PMA design, i.e., the **Pleated Pneumatic Artificial Muscle (PPAM)**, is created by Daerden at the Vrije University Brussel [6].

Figure 4.3: Example of PPAM [24]

This design consists of a membrane which is arranged into radially laid out folds. This feature allows a free unfurling without radial stress. Figure 4.3 illustrates the working principal of a PPAM. This artificial muscle operates from 20 mbar to 4 bar and reaches contraction until 40%, depending on the nominal length of the muscle. With a weight of 100 g is the PPAM able to generate forces up to 5 KN.
The force-contraction characteristic of a PPAM depends on the slenderness and the nominal length of the muscle. In comparison, a McKibben muscle is characterized by its diameter.

McKibben muscles are commercialized by different brands for example Festo, Shadow or Merlin. The **Festo fluidic muscles** are the most widely used McKibben muscles. The Figure 4.4 shows a visual of the fluidic muscle as marketed by Festo which are available in different diameters and lengths and are able to generate a maximum force up to 5 kN at 6 Bar.

Figure 4.4: Festo Fluidic Muscle [10]

On comparing both muscles, we find that the fluidic muscles by Festo are able to operate at higher pressures of 6 bar for DMSP-20. In Figure 4.5 can be seen a comparison of the contraction at same forces of the two muscle types. While Festo muscles are limited to 25%, PPAMs reach a practical contraction over 38%.
The next noticeable difference between the muscles is the elasticity. Festo muscles elongate slightly in their pretensioned state due to their elastic components, whereas PPAMs are rigid because of the in-elasticity of the fibres.

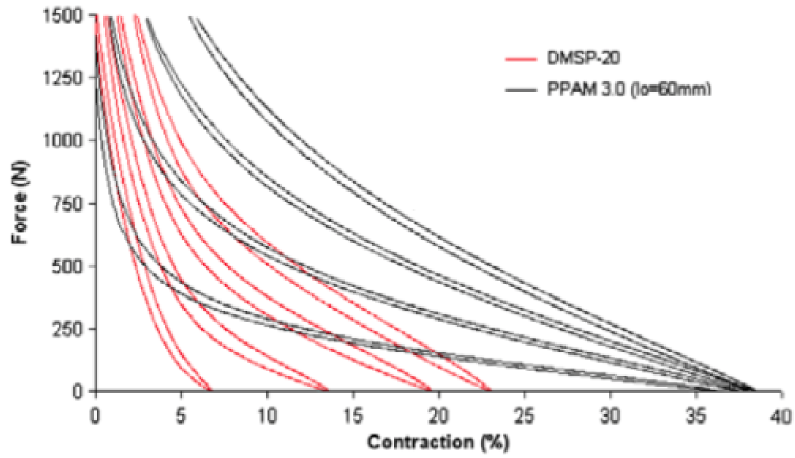

Figure 4.5: Comparison of contraction of PPAM and Festo poducts [24]

As already seen in previous figures, the inflation of the muscles are different. While the shell structure of the Festo muscle keeps the tube in a cylindric shape during the inflation, PPAM deforms completely and ends in a shape of a spheroid. Therefore, the diameter of a PPAM is usually more as doubled from initial state to inflated state.

		Festo Fludic Muscle			PPAM		
Properties	Units	DMSP-10-40	DMSP-20-60	DMSP-40-120	lo=40mm	lo=60mm	lo=120mm
Max Tension	N	630	1500	6000	660	1487	5950
Max Diameter	mm	20.7	39	75.4	35.4	53	106.1
Max contraction	%	13	22.8	28.3	38.2	38.2	38.2
Tension intensity	kN/m^2	1526.3	1255.6	1473.6	618.2	618.2	618.2
Force to Mass	kN/kg	8	7.1	7.4	9.8	19.7	50.2
Energy to Mass	Nm/kg	14.6	38.7	108.1	72.7	218.5	1112
Energy to Volume	Nm/l	268.5	159.1	227.8	287.1	287.1	287.1

Table 4.1: Concluding comparison table [24]

On comparing the properties of the two muscles as shown in Table 4.1, we find that while the PPAM is more compact and lightweight, its diameter increases significantly compared to the fluidic muscle of Festo. Therefore, Festo muscles are able to work close to the robot structure which enables a more compact design. Furthermore, the elasticity of the thin muscles creates a compliance of the actuation of the device.

Festo Fludic Muscle

Festo developed 2009 a the new pneumatic drive, the Fluidic Muscle [10], which enables sequences that approximate human movements. It consists of an elastomer cylinder embedded with aramid fibres. The contraction of the muscle is created by the entering compressed air. The internal name for the product is DMSP/MAS (depending on the attachment type) followed by the nominal length and diameter of the muscle. The product characteristics are only depended on the diameter of the muscle which can be seen in Figure 4.6.

Fluidic Muscle	Operating pressure	Max. clamping force/ outside Ø
DMSP-5	6 bar	**140 N/11 mm**
DMSP-10	8 bar	**630 N/22 mm**
DMSP-20	6 bar	**1500 N/35 mm**
DMSP-40	6 bar	**6000 N/57 mm**

Figure 4.6: Characteristics of Festo Muscles [10]

Festo provides different peripherals for connecting to a structure which can be seen in Figure 4.7.

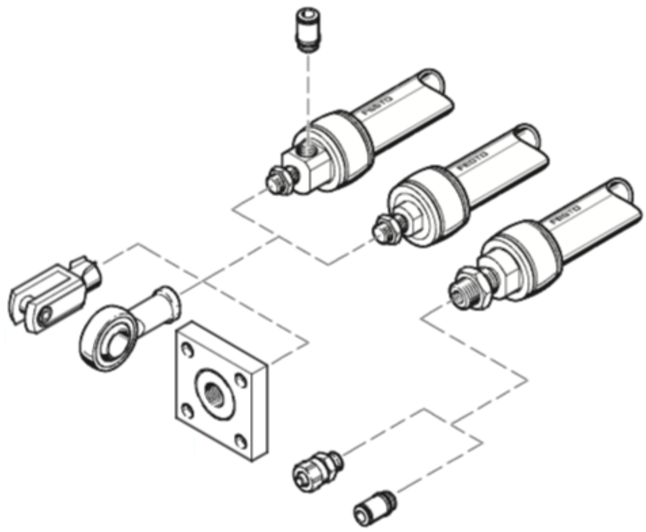

Figure 4.7: Peripheral overview of connectors [10]

Figure 4.8 illustrates the force-contraction relationship of an example muscle with different air pressures. This graph shows that the muscle loses maximum applicable force over increasing contraction.

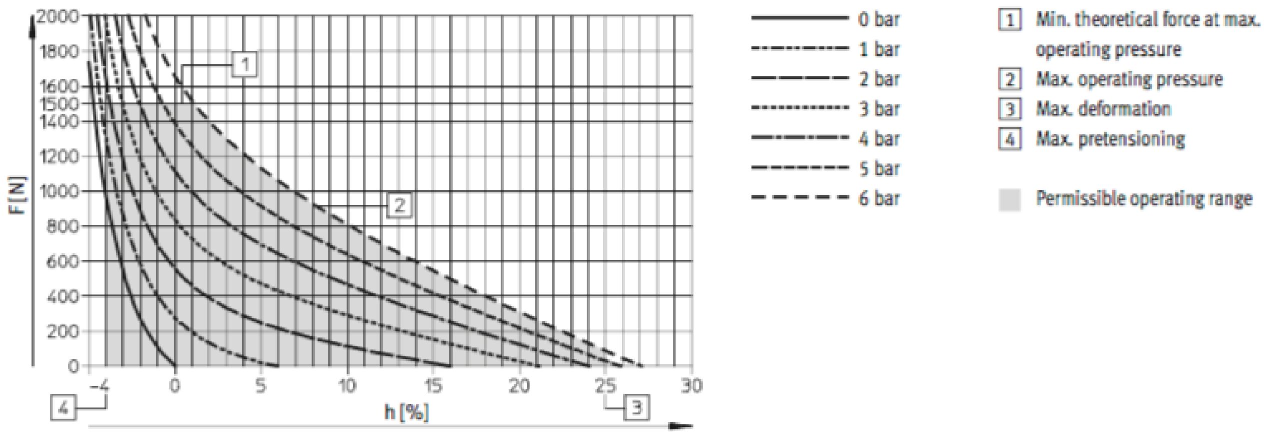

Figure 4.8: Force-Contraction characteristic of DMSP-20 [10]

4.4 Calculations

Before the created concept can be constructed, we calculate the scale required for the actuators. The results of these calculations are further inserted into the developed design to show the functioning of the device. Before the strains and torques can be determined, the **desired weight** has to be set.

As mentioned in the Background section, the statistical RMS torque value of the elbow joint in ADLs is assumed with $\tau_{stat} = 1{,}4Nm$.
Due to the simplifications and the neglect of any frictions and inertia, a **safety factor (SF) of 20** was chosen.

$$\tau_{lift,max} = SF \cdot \tau_{stat} = 20 \cdot 1{,}4Nm = 28Nm \tag{4.2}$$

With Equation 3.6, the maximum lifting weight can be established. Previously, the statistical length and weight of the human forearm have to be assumed. The National Technical Information Service in Springfield, USA has been represented statistical parameter of the human body [5], where $m_f = 1{,}1kg$ and $r_{EH} = 0{,}3m$. The mass of the arm is simplified in the middle of the arm.

$$m_w = \frac{\tau_{lift,max} - m_f g(r_{EH} - r_{f,x})}{g r_{EH}} = \frac{28Nm - 1{,}1kg \cdot 9{,}81m/s^2 \cdot (0{,}3m - 0{,}15m)}{9{,}81m/s^2 \cdot 0{,}3m} = 8{,}97kg \tag{4.3}$$

Equation 4.3 results in a **maximum lifting weight of 8.97 kg**.

In order to scale the PMAs, the maximum strain force is required which will define the diameter of the muscle.

$$f_{max} = \frac{\tau_{lift,max}}{r_{EA}}, \tag{4.4}$$

where r_{EA} represents the distance between the fulcrum and the attached muscle. The arrangement of the fulcrum and the attached muscle is illustrated in Figure 2.5. The distance r_{EA} depends on the geometric characteristic of the simulated device.

4.4.1 Scaling of Festo Fluidic Muscle

In order the scale the muscle, the contraction and the maximum load has to be established as followed:

Nominal and Maximal Length

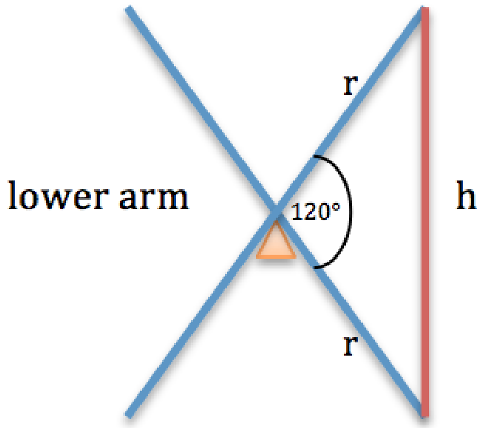

Figure 4.9: Simplification for calculation the contraction

Since the simplification (shown in Figure 4.9) is an isosceles triangle with a main angle of 120° (maximum angle of rotation), h can be calculated using the sine law:

$$h = r \cdot \frac{\sin(120°)}{\sin(30°)} = 24 \cdot \frac{\sin(120°)}{\sin(30°)} = 41{,}56mm, \tag{4.5}$$

where r represents the distance between the muscle attachment and the fulcrum which is set at $24mm$. Once the contraction is known, the required nominal length of the muscle can be determined as:

$$l_{nominal} = h : 25\% = 41{,}56mm : 25\% = 166{,}24mm \tag{4.6}$$

Finally the Festo Fluidic Muscle is set to a **nominal length of 165 mm**. Consequently the maximum distance between the attachments can be evaluated by adding the lengths of the connectors and attachments (Figure 4.10) for the muscle:

$$l_{max} = l_{nominal} + 2 \cdot connector + 2 \cdot attachment = \\ 165mm + 2 \cdot 47{,}5mm + 2 \cdot 40mm = 340mm \tag{4.7}$$

The maximal length of the muscle is needed as a parameter for the constructed device which is set to $340mm$.

Maximum Load

Once the maximum lifting torque $\tau_{lift,max}$ and the distance r between the fulcrum and the attached muscle r are known, the maximum force can be calculated with the Equation 4.4:

$$f_{max} = \frac{28Nm}{0{,}024m} = 1166,67kN \tag{4.8}$$

We look up the largest force lower than f_{max} in Table 4.6 to determine the diameter and nominal length of the muscle. We find that for the obtained force f_{max}, the muscle diameter should be $20mm$ and the nominal length should be $165mm$ and leads to the specific muscle **DMSP-20-165**.

4.5 Designed Device

As the last step of this research, a raw structure of the exoskeleton was developed with the 3D CAD software Autodesk Inventor.
The CAD-drawings of the Festo Fluidic Muscle and the needed attachments are provided by Festo [10].

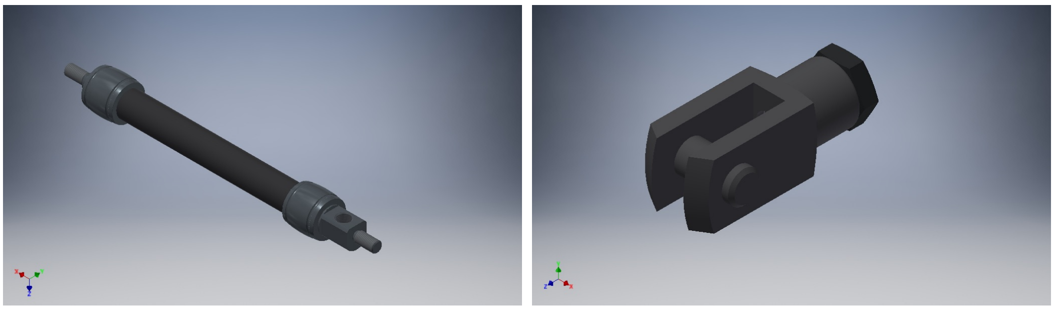

(a) Festo Fludic Muscle (b) Attachment

Figure 4.10: CAD-Drawings provided by Festo

The exoskeleton structure is separated into a lower and upper part and connected with a joint which is as close to the human elbow joint as possible (Figure 4.11). Additionally, the maximum muscle length is guaranteed using the enhancement on the top of the upper part.

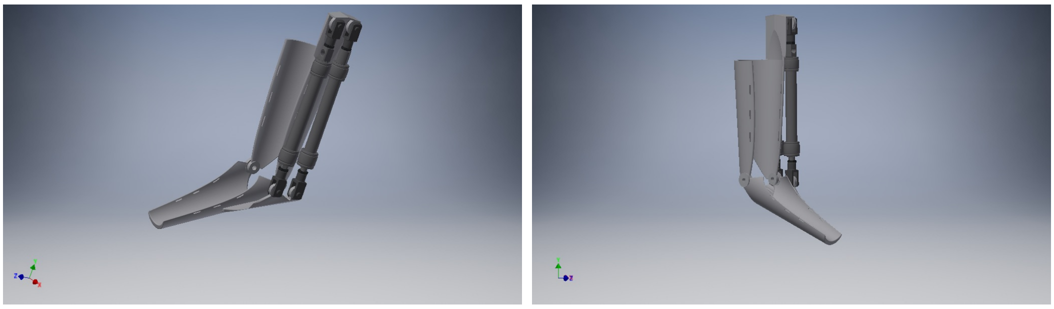

(a) rigth perspective (b) left prespective

Figure 4.11: Whole device in neutral position

The maximum flexion and extension is limited by the contraction of the muscles calculated in the previous section. As illustrated in Figure 4.12, the exoskeleton can be manipulated from 10° to 130°.

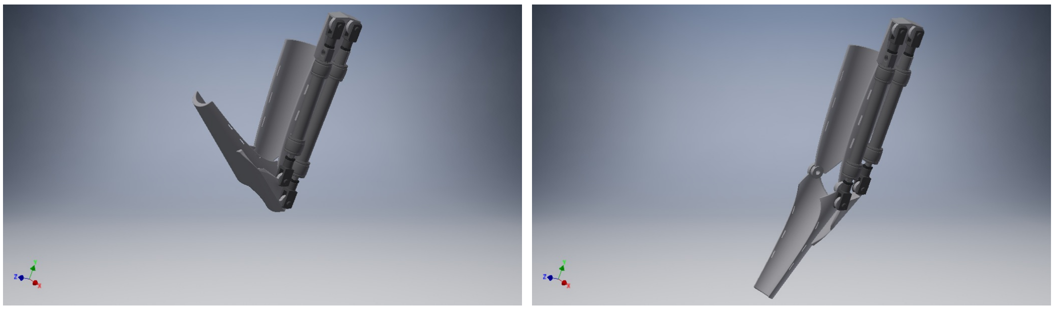

(a) flexioned (b) extensioned

Figure 4.12: Whole device in maximum positions

In order to fasten the new structure to the human arm, hook and loop fastener have to be attached on the side holes as seen in Figure 4.13.

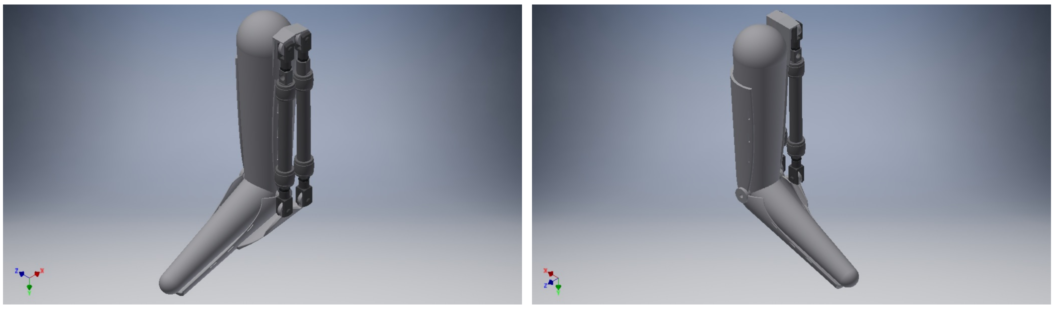

(a) right perspective

(b) left perspective

Figure 4.13: Whole device with human arm

4.6 Discussion

In this chapter, different actuators and sensor designs were discussed and explained. The EMG detection system detects muscle signals, process them and uses additional force sensors for driving the actuators. The used actuators are compliant and humanlike which were realized with Festo Fluidic Muscle. These muscles were scaled with the set dimension and forces. Finally, the device is constructed with a 3D CAD software to get a overview of the structure.

Chapter 5

Discussion

5.1 Conclusion

In order to support people with muscle weaknesses or illnesses in daily live, a new concept of compliant exoskeleton has to be developed. While commercial assistive robots are available, several robots have disadvantages such as stiffness or complexity of use. Additionally, the main criteria are usually not fulfilled by these commercialized products which includes the fully control of the user over his/her movement or the effect of compliance.

This literature research presents a new sophisticated concept of an compliant exoarm for daily life activities. Furthermore, the background knowledge, which consists of the physical design and the action of movement of a human arm, has been summarized to understand the principal behavior and function of the human arm as well as the statistical loads and torques during different activities in daily lives (ADL). The first chapter contains the principle of creating a movement by contracting a muscle which can be detected by an EMG sensor.
In Chapter *3.1.1* current human-robot-interactions (HRIs) and actuators were summarized with a respectively discussion about the capability of the particular principals which resulted in the use of a EMG detection system due to the broad application range while the exosarm is driven by pneumatic muscle actuators (PMAs). Before analyzing the PMAs in detail, two different principals of the pneumatic muscle, McKibben muscle commercialized by Festo and planted pneumatic artificial muscle (PPAM), were compared. Both mus-

cles have the same force-ranges, but the Festo Fluidic Muscle does not inflate during compression, which enables the attachment to remain close to the exoskeleton structure. Therefore, the Festo Fluidic Muscle was evaluated in more detail. Based on these decisions, state-of-the-art concepts of exoskeletons were assessed and compared. Two concepts were presented which fit best with the desired aim: RUPERT and MyoPro. By combining the main advantages of both concepts, i.e., the EMG detection system of MyoPro and the PMA drive of RUPERT, a new compliant exoarm was developed.
Since a raw structure has been fixed, calculations were conducted to scale the PMA developed by Festo. These calculations began by computing the required torque with a safety factor and followed by establishing the maximum lifting weight. The last step included the development and construction of the new design of the exoarm in the 3D CAD software Autodesk Inventor. This 3D sketch creates a raw overview of the design and the working principal of the new compliant exoskeleton.

5.2 Future

Based on the results of the presented research a simulation and a prototype can be developed for proving the functionality of the design. This includes the decision which materials fits best for the exoskeleton structure. Furthermore, to ensure the purposed function of the exoarm, the data processing and the controlling of the actuators has to be built which could include one of the presented devices for converting the measured raw EMG signal. For driving the actuators, the nonlinear characteristic has to be taken into account to ensure an accurate movement.

Lastly, experiments and tests can be established to prove the desired functionality of the compliant exoarm.

List of Figures

List of Tables

Bibliography

[1] Alexandra: *Lever of Human Body*. https://alexeinstein.wordpress.com/2014/09/03/lever-of-human-body/.

[2] Baklouti, Malek, Eric Monacelli, Vincent Guitteny and Serge Couvet: *Intelligent Assistive Exoskeleton with Vision Based Interface*. In Helal, Sumi, Simanta Mitra, Johnny Wong, Carl K. Chang and Mounir Mokhtari (editors): *Smart Homes and Health Telematics*, number 5120 in *Lecture Notes in Computer Science*, pages 123–135. Springer Berlin Heidelberg.

[3] Balasubramanian, Sivakumar, H. Ruihua Wei, Mike Perez, Ben Shepard, Edward Koeneman, James Koeneman and Jiping He: *Rupert: An exoskeleton robot for assisting rehabilitation of arm functions*. In *2008 Virtual Rehabilitation, IWVR, August 25, 2008 - August 27, 2008*, 2008 Virtual Rehabilitation, IWVR, pages 163–167. Inst. of Elec. and Elec. Eng. Computer Society.

[4] Brody, G., R. N. Scott and R. Balasubramanian: *A model for myoelectric signal generation*. 12(1):29–41.

[5] Clauser, Charles E, John T McConville and John W Young: *Weight, volume, and center of mass of segments of the human body*. Technical Report, DTIC Document, 1969.

[6] Daerden, Frank: *Conception and realization of pleated pneumatic artificial muscles and their use as compliant actuation elements*. PhD Thesis Vrije Universiteit Brussel, Belgium, 7:2O, 1999.

[7] De Rossi, D., F. Carpi, F. Lorussi, E.P. Scilingo and A. Tognetti: *Wearable kinesthetic systems and emerging technologies in actuation for upperlimb neurorehabilitation*. In *Annual International*

Conference of the IEEE Engineering in Medicine and Biology Society, 2009. EMBC 2009, pages 6830–6833.

[8] Denavit, Jacques: *A kinematic notation for lower-pair mechanisms based on matrices.* Trans. of the ASME. Journal of Applied Mechanics, 22:215–221, 1955.

[9] Dutton, Mark: *Chapter 17. Elbow.* In *Dutton's Orthopaedic Examination, Evaluation, and Intervention.* McGraw-Hill Education, Third Edition edition.

[10] Festo, AG and Co. KG: *Festo Fluidic muscle.* https://www.festo.com/group/en/cms/10248.htm, 2009.

[11] Halabi, Osama and Haruhisa Kawasaki: *Five Fingers Haptic Interface Robot HIRO: Design, Rendering, and Applications.* In Hosseini, Mehrdad (editor): *Advances in Haptics.* InTech.

[12] Kajitani, I., M. Murakawa, D. Nishikawa, H. Yokoi, N. Kajihara, M. Iwata, D. Keymeulen, H. Sakanashi and T. Higuchi: *An evolvable hardware chip for prosthetic hand controller.* In *Proceedings of the Seventh International Conference on Microelectronics for Neural, Fuzzy and Bio-Inspired Systems, 1999. MicroNeuro '99*, pages 179–186.

[13] Kapur, P., S. Premakumar, S.A. Jax, L.J. Buxbaum, A.M. Dawson and K.J. Kuchenbecker: *Vibrotactile feedback system for intuitive upper-limb rehabilitation.* In *EuroHaptics conference, 2009 and Symposium on Haptic Interfaces for Virtual Environment and Teleoperator Systems. World Haptics 2009. Third Joint*, pages 621–622.

[14] Kerscher, Thilo, Jan Albiez, JM Zöllner and Rüdiger Dillmann: *Evaluation of the dynamic model of fluidic muscles using quick-release.* In *Biomedical Robotics and Biomechatronics, 2006. BioRob 2006. The First IEEE/RAS-EMBS International Conference on*, pages 637–642. IEEE, 2006.

[15] Kiguchi, K. and Y. Hayashi: *An EMG-Based Control for an Upper-Limb Power-Assist Exoskeleton Robot.* 42(4):1064–1071.

[16] Lo, Ho Shing and Sheng Quan Xie: *Exoskeleton robots for upper-limb rehabilitation: State of the art and future prospects.* 34(3):261–268.

[17] Myomo, Inc.: *MyoPro Myoelectric Upper Limb Orthosis.* http://www.myopro.com, 2015.

[18] Paul R., Shimano B.: *Compliance Control.* Proceedings of the JACC.

[19] Perry, J.C., J. Rosen and S. Burns: *Upper-Limb Powered Exoskeleton Design.* 12(4):408–417.

[20] Raez, M.B.I., M.S. Hussain and F. Mohd-Yasin: *Techniques of EMG signal analysis: detection, processing, classification and applications.* 8:11–35.

[21] Salisbury, J.K.: *Active stiffness control of a manipulator in cartesian coordinates.* In *1980 19th IEEE Conference on Decision and Control including the Symposium on Adaptive Processes*, pages 95–100.

[22] Stone, William C: *Electroactive Polymers as Artificial Muscles: Capabilities, Potentials and Challenges.* In *Robotics 2000*, pages 188–196. American Society of Civil Engineers, 2000.

[23] Sugar, T.G., Jiping He, E.J. Koeneman, J.B. Koeneman, R. Herman, H. Huang, R.S. Schultz, D.E. Herring, J. Wanberg, S. Balasubramanian, P. Swenson and J.A. Ward: *Design and Control of RUPERT: A Device for Robotic Upper Extremity Repetitive Therapy.* 15(3):336–346.

[24] Villegas, Daniel, Michael Van Damme, Bram Vanderborght, Pieter Beyl and Dirk Lefeber: *ThirdGeneration Pleated Pneumatic Artificial Muscles for Robotic Applications: Development and Comparison with McKibben Muscle.* 26(11-12):1205–1227.

[25] Widmaier, Eric P., Hersel Raff and Kevin T. Strang: *Vander's Human Physiology: The Mechanisms of Body Function.* McGraw-Hill, 12th edition.

[26] Wu, Tzong-Ming, Shu-Yi Wang and Dar-Zen Chen: *Design of an exoskeleton for strengthening the upper limb muscle for overextension injury prevention.* Mechanism and Machine Theory, 46(12):1825–1839, December 2011. bibtex: wu_design_2011.

[27] Yen, Chih-Jen, Wen-Yaw Chung, Kang-Ping Lin, Cheng-Lun Tsai, Shing-Hao Lee and Te-Shin Chen: *Analog integrated circuit*

design for the wireless bio-signal transmission system. In *The First IEEE Asia Pacific Conference on ASICs, 1999. AP-ASIC '99*, pages 345–346.